Anbar Journal of Engineering Science (AJES) **Vol. 12 , No. 2 (2021) , pp.** 245 ~ 255
P-ISSN: 1997-9428; E-ISSN: 2706-7440 DOI:10.37649/aengs.2021.171192

Anbar Journal Of Engineering Science©

journal homepage: http://www.uoanbar.edu.iq/Evaluate/

Unviersty of Anbar

Artificial Neural Networks Modeling of Heat Transfer Characteristics in a Parabolic Trough Solar Collector using Nano-Fluids

T. A. Salih, S. A. Mutlag, H. K. Dawood

Mechanical Engineering Department, College of Engineering, University of Anbar, Ramadi, Anbar, Iraq

PAPER INFO

Paper history:
Received 10/10/2021
Received in revised form 16/11/2021
Accepted 22/11/2021

Keywords:
Solar thermal performance, Parabolic trough solar collector, Artificial neural network, CuO/H_2O nano-fluids, TiO_2/H_2O nano-fluids.

ABSTRACT

In the current article, an experimental investigation has been implemented of flow and heat transfer characteristics in a parabolic trough solar collector (PTSC) using both nano-fluids and artificial neural networks modeling. Water was used as a standard working fluid in order to compare with two different types of nano-fluid namely, nano-CuO /H_2O and nano-TiO_2/ H_2O, both with a volume concentration of 0.02. The performance of the PTSC system was evaluated using three main indicators: outlet water temperature, useful energy and thermal efficiency under the influence of mass flowrate ranging from 30 to 80 Lt/hr. In parallel, an artificial neural network (ANN) has been proposed to predict the thermal efficiency of PTSC depending on the experimental results. An Artificial Neural Network (ANN) model consists of four inputs, one output parameter and two hidden layers, two neural network models (4-2-2-1) and (4-9-9-1) were built. The experimental results show that CuO/ H_2O and TiO_2/H_2O have higher thermal performance than water. Overall, it was verified that the maximum increase in thermal efficiency of TiO_2/H_2O and CuO/H_2O compared to water was 7.12% and 19.2%, respectively. On the other hand, the results of the model 4-9-9-1 of ANN provide a higher reliability and accuracy for predicting the Thermal efficiency than the model 4-2-2-1. The results revealed that the agreement in the thermal efficiency between the ANN analysis and the experimental results about of 91% and RMSE 3.951 for 4-9-9-1 and 86% and RMSE 5.278 for 4-2-21.

1. Introduction

In today's environment, the phrases "nano" and "energy" are two globally attractive keywords. Due to a significant great in fossil fuel consumption, renewable energy has also gained a lot of traction. In other words, environmentalists want renewable energy sources to replace fossil fuels [1]. However, despite some limitations in terms of stability and cost, nano-fluids are widely used in a wide range of solar heating and cooling systems, including combined cooling, heating, and power (CCHP) stations, water heating systems, heat pumps, and desalination systems, to improve the efficiency of solar systems [2,3]. In addition, a modelling of solar systems has usually been dispensed standardly [4]. In anoth-

* Corresponding author. : T. A. Salih : t.salih@uoanbar.du.iq ; +9647824337889

er hand, there exist some various approaches that predict the potency of the system even additional accurately than the simplest conventional modelling approaches of solar systems, comparable to artificial neural network, genetic programming, genetic algorithm and different promising machine learning primarily based approaches. Safarzade et al. [5] improved the thermal efficiency of PTSC through the use of Cu_2O /H_2O nano-fluid and a parabolic concentrator that can achieve the thermal efficiency of the solar system up to 12%. In addition, the effect of different concentrations of nanoparticles on the thermophysical performance of Liquid Iacobazzi et al. [6] made a receiver with a parabolic groove. They managed to achieve 11% thermal efficiency of the solar system using a mixture of CuO nanopowder and air. Favale et al. [7] used nano-fluid Al_2O_3 to improve the energy efficiency of heat exchangers for cooling electronic devices. The factors of stability of nano-fluid Al_2O_3 and the effect of surfactants on its thermal conductivity were evaluated. The results showed that the temperature when the nano-fluid was being created boosted the thermal efficiency of the solar system by up to 13%, according to the authors. The thermal conductivity of Al_2O_3 nano-fluid is reduced more by differences in mass dispersion than by other parameters including thermal boundary resistance, Brownian motion, clustering, and layering, according to Milanese et al. [8]. With the use of an artificial neural network (ANN), Boutella et al. [9] were able to forecast and optimize the levelized electricity cost of two separate thermal power plants with two different working fluids. Kalogirou [10] employed Artificial Neural Networks to forecast flat plate solar collector performance characteristics. The results showed that the ANN method could forecast the solar system's significant thermal parameters more precisely than traditional methods of modeling solar systems. Burrati et al. [11] used Artificial Neural Network modeling to verify the accuracy of certificates connected to building energy usage in Italy. Tomy et al. [12] used an Artificial Neural Network (ANN) to predict the efficiency of a flat plate solar collector with Ag/H_2O nano-fluid. Reynold's estimate ranged from 5000 to 25,000. The findings matched the experimental inquiry perfectly. Mahian et al. [13] conducted a mathematical analysis of the effect of nanoparticle volume percentage in base fluid and nanomaterial form on the second law efficiency of thermal solar systems in 2014.The thermal properties of a manufactured PTSC and the utilization of TiO_2/H_2O and CuO/ H_2O nano-fluid are studied in this study. To ensure the correctness of the Artificial Neural Network prediction modeling, the input data are taken from experimental investigations, and the results obtained from the experimental data are compared to those of the expected outcomes. Finally, the thermal properties of the best PTSC at various mass flow rates are studied.

2. Experimental set-up

Fig. 1 depicts a picture of the adopted experimental protocols, along with a short description of each component. The experimentations were carried out in Ramadi at longitude (32.559 ˚N and 41.9196 ˚E) during selected days from January 2021 to February 2021. The nano-fluid was prepared for volume concentrations (0.02 vol). As illustrated in Fig. 1, the PTSC setup contains smooth absorber tube, storage tank with volumes of 31.5 Lt, a curved Nichol- Chrom sheet as the parabolic concentrator used as concentrator, a cast iron frame to lessen the weight of the collector for more convenient maintenance. Because the experiments were conducted in the winter and the azimuth angle was high, the collector should be positioned at angles less than the latitude of the researched location. The collector was tilted at a 35° angle. According to a similar study [5], thermocouples are connected to a data logger type GM4208 manufactured by Lutron Collaboration. The characteristics of the designed configuration are shown in Table 1. At the end of each day of the experiment, all the working fluid was evacuated inside the PTSC, and the next morning a new flow was changed so that the previous residue did not affect the experiment. In progress, the data was recorded half an hour before the start of the thermal studies (starting at 8:30 am) to exclude temperature fluctuations from the yield estimates. Solar insulation is measured every minute with a TES132 solar meter. The experiments were carried out from 9 am at 15:00.

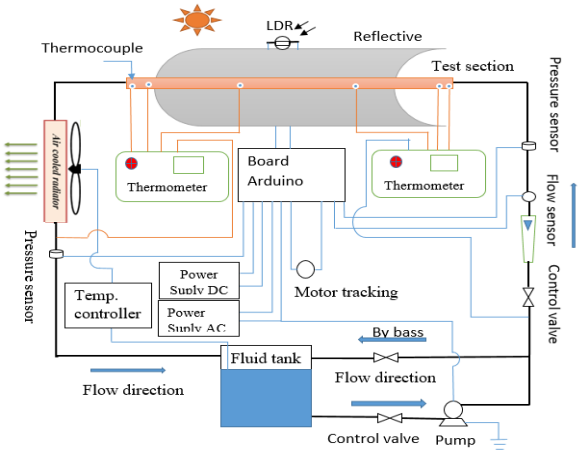

Figure 1. Schematic diagram of experimental set-up.

Table 1. Characteristics of the experimental setup.

Part	Specifications
Collector aperture width	1.0 m
Collector length	2.0 m
Aperture area	2.0 m^2
Rim angle	90̊
Focus length	0.24m
Concentration ratio	14.
Mod of tracking	Two axes
Tracking mechanism type	Electro-optical
Reflector material	Nickel- Chrom sheet
Receiver material	Copper
Receiver length	2.10 m
Receiver inner diameter	0.0223 m
Receiver outer diameter	0.023 m
Thermal conductivity of copper	400 W/m. K
Coolant	Water, TiO_2/Water and CuO /Water
Tank material / capacity	Galvanize sheet / 31.5 Lt
Water pump	120 W
Support Structure material	Iron

3. Nano-fluid

In order to prepare the nano-fluid with a volume concentration of 0.02, with an average diameter of 30 nm and a purity of 99.99% for CuO, TiO_2 was used. The mass of the required nanoparticles that is proportional to the specific volumetric concentration is first calculated using the following equation [14].

$$\varphi\% = \frac{\left[\frac{w_p}{\rho_p}\right]}{\left[\frac{w_p}{\rho_p}+\frac{w_{bf}}{\rho_{bf}}\right]} \quad (1)$$

$$W_p = \rho_p \left[\frac{\emptyset}{1-\emptyset}\right]\left[\frac{W_f}{\rho_f}\right] \quad (2)$$

Then the weight of the nanoparticles mass is measured using a high-precision digital scale, then mix the nano powder with distilled water, and the amount of distilled water is proportional to the number of nanoparticles calculated in Table 2. The mixing of nanoparticles with distilled water lasted for 1 hour under an Ultra-Sonicator, the frequency of which was 60 kHz during a half hour period of time as illustrated in Fig. 2. The above process is repeated until we reach the required volume (17 liters) of the nano-fluid. The prepared stable solution was then kept under ultrasonic vibration frequency again for better stabilization purposes for the same duration. The nano-fluid was used in this experimental investigation after two days of preparation.

Table 2. Volume concentrations and weight of nanoparticles

Volume concentrtions (Ø), %	TiO_2 /H_2O (g)	CuO/H_2O (g)
0.02%	0.4231	0.63113

(a) (b)

Figure. 2 The process of nano-fluids preparation, (a) CuO/H_2O and (b) TiO_2 /H_2O.

3.2. Nano-fluid thermophysical properties

The thermophysical properties of pure H_2O, various base fluids and various nanoparticles which are heat capacity, density, effective dynamic viscosity; effective thermal conductivity and thermal expansion coefficient are given in Table 2. The following equations are used to calculate the density, specific heat, viscosity, and thermal conductivity of the TiO_2/H_2O and CuO/H_2O nanofluid is produced by [15]:

$$\rho_n = (1-\varphi)\,\rho_f + \varphi\,\rho_p \quad (3)$$

$$C_{p,n} = ((1-\varphi)\,(\rho\,C_p)_f + \varphi\,(\rho\,C_p)_p)\,\rho_n \quad (4)$$

$$\frac{\mu_{eff}}{\mu_f} = 1 + 2.5\,\varphi \quad (5)$$

$$\frac{K_{nf}}{K_f} = \frac{(K_p+2K_f+2\varphi\,(K_f-K_p))}{K_p+2K_f+\varphi\,(K_f K_P)} \quad (6)$$

Finally, the thermophysical properties of nanoparticles and water at T= 300 K are presented in Table 3

Table 3. Volume concentrations and weight of nanoparticles [16].

Thermo physical	ρ (kg/m^3)	Cp (J/kg.k)	K (W/m.k)
TiO_2	4230	686.2	8.95
Water	996.5	4181	0.613
CuO	6500	533	17.65

4. Data reduction

In this section, the general experimental data that has been obtained will be reduced for computing the required results. In the PTSC, the solar radiation intensity (I) is gained and thus the solar irradiation through the collector apparatus (Qs) is calculated as [17]:

$$\mathbf{Q}_s = \mathbf{A}_a \mathbf{I} \quad (7)$$

$$\mathbf{A}_a = (\mathbf{W}_a - \mathbf{d}_{ro})\,\mathbf{H}_p \quad (8)$$

The Qu captured by the fluid is calculated according to

$$Q_u = m \cdot C_p (T_{out} - T_{in}) \quad (9)$$

$$m = \rho V \quad (10)$$

The ηth of the PTSC system is defined as [18]:

$$\eta_{th} = \frac{Q_u}{Qs} \quad (11)$$

$$A_{ri} = \pi\, d_{ri}\, L \quad (12)$$

$$\mathbf{T_m} = \frac{(\mathbf{T_{in}} + \mathbf{T_{out}})}{\mathbf{2}} \quad (13)$$

The Renolds number is determined as following:

$$Re = \frac{\rho\, U_m d_{ri}}{\mu} = \frac{4\,\dot{m}}{\pi\, d_{ri}\, \mu} \quad (14)$$

$$Ac = \frac{\pi\, d_{ri}^2}{4} \quad (15)$$

5. Methdology of Artificial Neural Networks (ANN)

Artificial Neural Networks (ANNs) are precise modeling tools for recognizing the characteristics of complex and nonlinear systems, such as solar water heating systems (SWHs). There are numerous types of neural networks available, each of which can be used to solve a specific problem. The ANN networks are trained using MATLAB R2014 software [19].

A. The basic components of an artificial neural network

The general structure of artificial neural networks is formed as shown in Fig.3 and consisted from:

1. Input layer: It is the process of feeding the input data to receive it by the processing units of the neurons [20].
2. Output layer: This layer consists of processing units through which the final output of the neural network is output [21].
3. Hidden layer: This layer is located between the input layer and the output layer [22].
4. Weights: It is the communication links between the different layers of the neural network. It connects network layers together or units within each layer to other units through the weights associated with each interface [20].
5. Neurons: Neurons are the units that connected in different ways by giving the overall shape or architecture of the artificial neural network. Neurons follow a parallel processing system that resembles the functioning of the human brain [21].

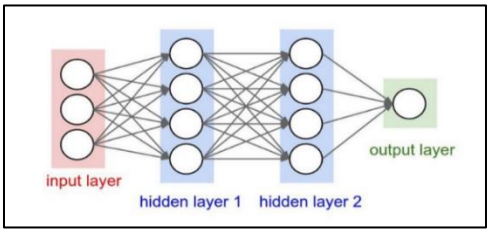

Figure 3. Artificial neural network architecture model [23].

Neural Network Structure: The ANN structure is made up of three layers: an input layer, a hidden layer, and an output layer, as shown in Fig.4The first hidden layer has I nodes, the second hidden layer has j nodes, and the output layer has one node. When applied to a single hidden layer, ANN is a 5-i-1, and when applied to two hidden layers, it is a 5-i-j-1. The number of nodes in the hidden layer is a function of the number of input nodes [24].

$$i \text{ or } j = \begin{cases} n/2 \\ n \\ 2*n \\ 2*n+1 \end{cases} \quad (16)$$

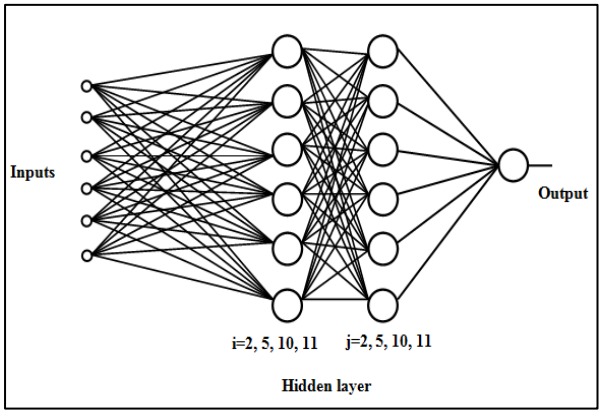

Figure 4. Network structures models.

B. Designing and Programming ANN Models

1- Designing ANN models:

A number of systemic approaches are used to create ANN models. There are five fundamental steps to follow in general: (1) data collection, (2) data preprocessing, (3) network building, and (4) training (5) testing and validation performance of model as shown in Figure 5.

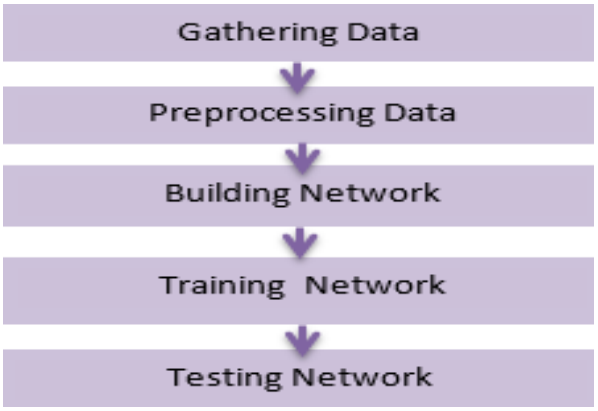

Figure 5. Basic flow for designing ANN model.

To begin, use MATLAB tools to develop an ANN. In both the hidden and output layers, our ANN is a Feed-Forward network with a tan-sigmoid transmission function. In this network, the hidden layer contains many of neurons. As the goal vector has three members, the network has five inputs and two outputs.

2) Data collection

After, using MATLAB tools, design an ANN. The initial stage in creating ANN models is to collect and prepare sample data. Tin, Tamb, Tr, and I were gathered using various instruments, as described in the previous section.

3) Data pre-processing

Three data preprocessing methods are carried out after data collection to improve the efficiency of the ANNs. The techniques are as follows: (1) fix the missing data problem, (2) normalize data, and (3) randomize data. The average of surrounding values from the same week is used to replace missing data. It is generally a good practice to perform a normalization procedure before presenting the input data to the network, as mixing variables with large and small magnitudes will confuse the learning algorithm as to the importance of each variable, causing it to reject the variable with the smaller magnitude.

4) Building the network

The number of hidden layers, neurons in each layer, transfer function in each layer, training function, weight/bias learning function, and performance function are all specified at this step. Feed-forward back prop network is used in this study.

5) Training the network

The weights are modified during the training phase to bring the network's actual (predicted) outputs closer to the network's target (measured) outputs. The training time for this study is three months, spanning January 2021 to February 2021. The linear (purelin), hyperbolic tangent sigmoid (logsig), and Logistic Sigmoid (logsig) transfer functions in MATLAB were used in this investigation (tansig). Table 4 shows the graphical representation of such functions as well as their mathematical form.

Table 4. Graphical representation,

Function Name	Graphical Illustration	Mathematical form
Linear	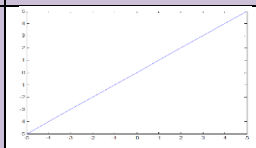	$f(x) = x$
Hyper-bolic Tangent Sigmoid	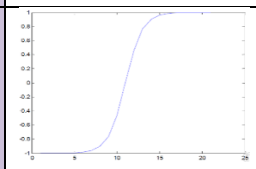	$f(x) = \frac{e^x - e^{-x}}{e^x + e^{-x}}$
Logistic Sigmoid	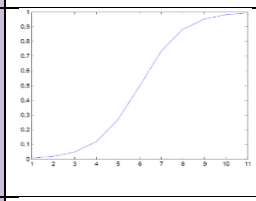	$f(x) = \frac{1}{1 + e^x}$
Gaussian RBF	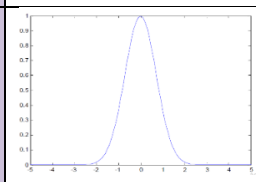	$\vartheta_j(x) = exp\left[-\frac{1}{2\,\vartheta_j^2}\|x - x_j\|_2\right]$

1) Testing the network

The next stage is to put the developed model to the test. The model gets exposed to previously unseen data at this point. Weather data from December 2020 to February 2021 was used to test the ANN models in the collector solar case study. On the other hand, a statistical analysis was undertaken to determine the correlation coefficient (R2), root mean square error (RMSE), and mean bias error (MBE) in order to quantify the performance of generated ANN models. There is a measure of variation in predicted values around measured data that provide information on short-term performance (RMSE). As the RMSE decreases, estimation accuracy increases. According to MBE, a model's long-term predictions are more accurate when there is a smaller average divergence between anticipated values and measured values. Similarly, a positive MBE value suggests that the anticipated GSR is overestimated, and vice versa. The expressions for the aforementioned statistical parameters are [25, 26]:

$$R^2 = 1 - \frac{\sum_{i=1}^{n}(\text{actual efficiency} - \text{predicted efficiency})^2}{\sum_{i=1}^{n}\text{predicted efficiency}^2} \quad (17)$$

$$\text{RMSE} = \sqrt{\frac{\sum_{i=1}^{n}(\text{actual efficiency} - \text{predicted efficiency})^2}{n}} \quad (18)$$

$$\text{MPE} = \frac{1}{n}\sum_{i=1}^{n}(\text{actual efficiency} - \text{predicted efficiency}) \quad (19)$$

$$\text{Error \%} = \frac{1}{n}\sum_{i=1}^{n}\frac{|\text{actual efficiency} - \text{predicted efficiency}|}{\text{actual efficiency}} \times 100 \quad (20)$$

Where n is the number of data samples that has been used in the experimental work.

6. Results and discussion

Nano-fluid fraction of nanoparticle 0.02 concentration of the experiments was conducted in order to summarize the findings and extract trends. Both experimental and predictid research have been conducted with the results split into two categories. Firstly, the effects of nano-fluid on the fluid's thermal properties have been explored, followed by comparisons of ANN optimization models and finally experimental thermal studies of the optimally designed PTSC.

6.1. Heat Gain with Time

The average heat gain became (448.4, 491.2, 594.5) watt for water, TiO_2/H_2O and CuO/H_2O respectively for the mass flow rate of 30 Lt/hr as shown in Fig.6.a, (440.3, 479.2, 582.94) watt for water, TiO_2/ H_2O and CuO/H_2O, respectively for a mass flow rate of 40 Lt/hr as shown in Fig. 6.b, (434, 463.8, 572.8) watt for water, TiO_2/ H_2O and CuO/H_2O respectively for a mass flow rate of 60 Lt/hr as shown in Fig.6.c and (388.9, 452, 554.3) watt for water, TiO_2 / H_2O and CuO/H_2O respectively for mass flow rate 80 Lt/hr as shown in Fig.6.d. the useful heat decreases with increasing flow, because the effect of the change between the inlet and outlet temperature of the fluid (ΔT) is greater than the effect of the flow, so that Qu will decrease in all cases when the flow increases.

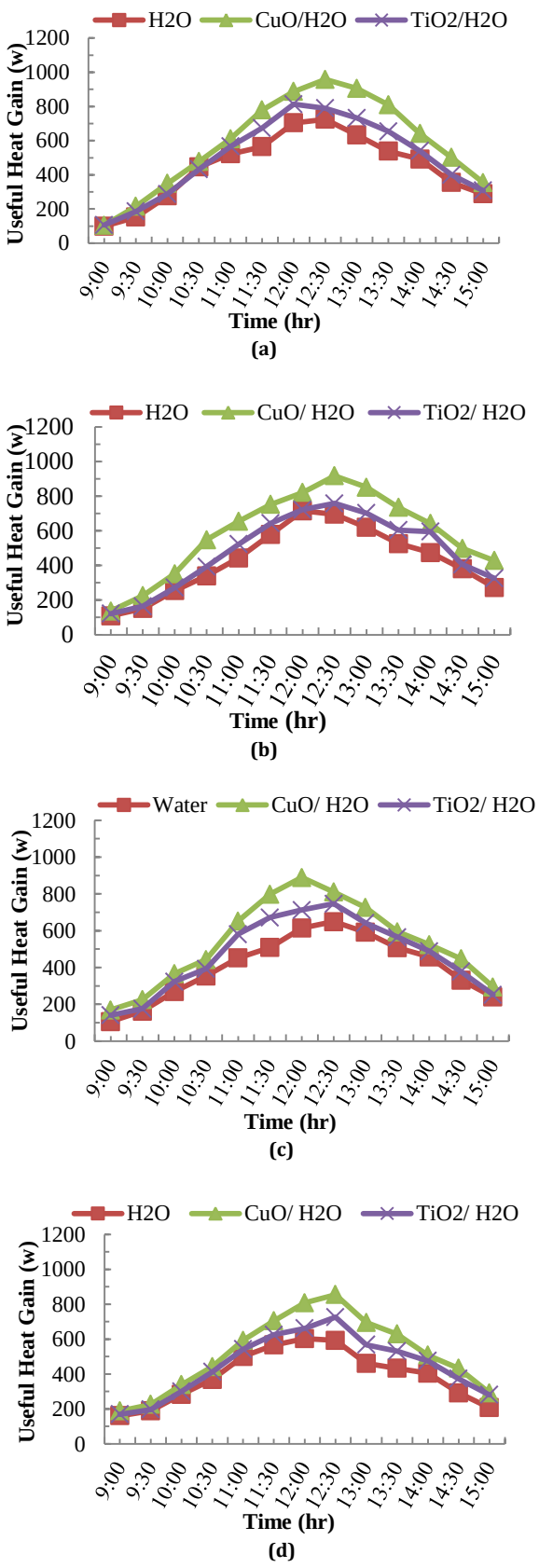

Figure 6. Useful heat gain versus time at (a) 30 Lt/hr, (b) 40 Lt/hr, (c) 60 Lt/hr, and (d) 80 Lt/hr.

6.2. *Efficiency with Time*

The average efficiency became (34.9, 32.2, 40.2) % for water, TiO_2/H_2O and CuO/H_2O respectively for the mass flow rate of 30 Lt/hr as shown in Figure 7.a, (33.6, 31.8, 42.1) % for water, TiO_2/H_2O and CuO/H_2O respectively for a mass flow rate of 40 Lt/hr as shown in Figure 7.b, (33.8, 31.9, 34.1) % for water, TiO_2/H_2O and CuO/H_2O respectively for a mass flow rate of 60 Lt/hr as shown in Fig.7.c and (29.8, 33.7, 38.5) % for water, TiO_2/H_2O and CuO/H_2O respectively for mass flow rate 80 Lt/hr as shown in Fig. 7.d.

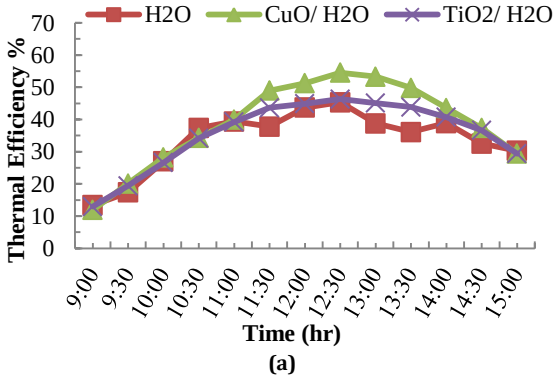

(a)

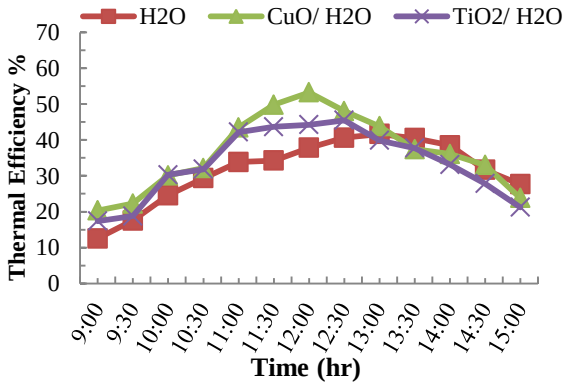

(b)

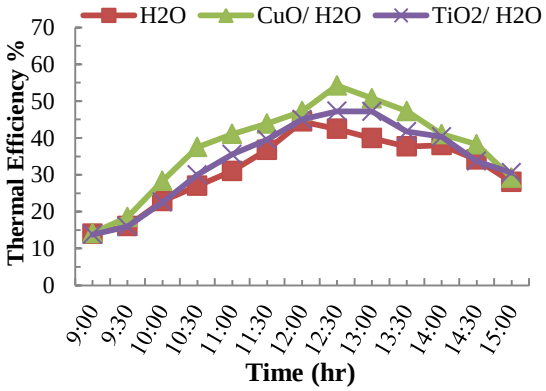

(c)

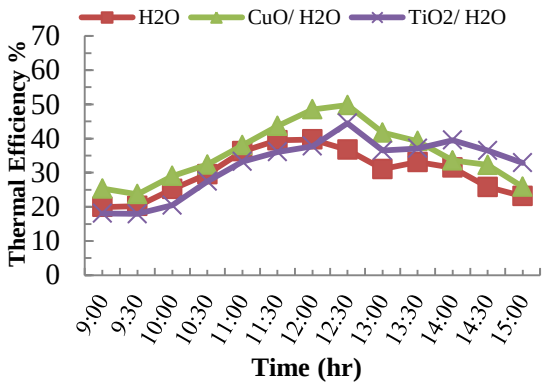

(d)

Figure 7. Efficiency versus time at (a) 30 Lt/hr, (b) 40 Lt/hr, (c) 60 Lt/hr, and (d) 80 Lt/hr.

6.3. *ANN Model Validation*

This section displays the best outcomes for ANN models that have been produced. The appropriate ANN topology training technique and number of neurons can be determined by using equation (17). When using the experimental data, the input layer parameters were derived from the logged operations. Receiver temperature (Tr), inlet fluid temperature (Tin), ambient temperature (Tamb) and sun intensity (I☼), were obtained. Over 156 data are used for training, and another 24 for validation and testing. There is only two hidden layers of the ANN architecture to estimate the best topology. The inlet fluid temperature (Tin), the receiver temperature (Tr), ambient temperature (Tamb), and sun intensity (I) are the input parameters used in the selected model. Thermal efficiency (η) is the output layers of the ANN. When it comes to the hidden and output layers of an artificial neural network, it is a feed-forward network with tan-sigmoid transmission function. In this paper, number of neurons, a neural network model containing the number of neurons, the Fig.8 shows the structure 4-2-2-1 and the Fig.9 shows the structure 4-9-9-1 was use in this work.

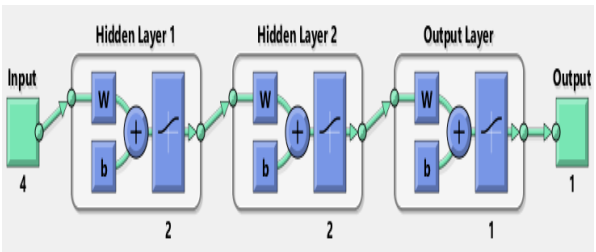

Figure 8. Structure(4-2-2-1) artificial neural network model.

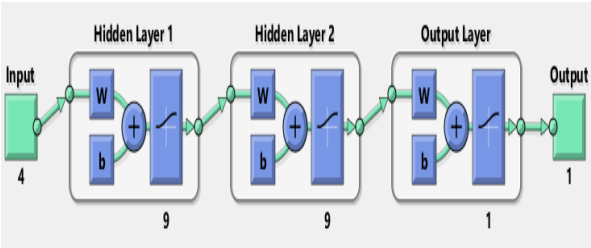

Figure9. Structure (4-9-9-1) artificial neural network model.

6.4. Predicting the Thermal efficiency

In Fig.10, The best training performance is 0.040726 at epoch 68 for 4-2-2-1 neural network architecture. The 4-9-9-1 neural network architecture, which was trained, shows that the best thermal efficiency prediction model with the best performance validation is 0.0049769 at epoch 178 as shown in Fig.11.

The comparison between the experiment data and the structure of the trained neural networks (ANN) (4-2-2-1) showed that the average percentage of thermal efficiency difference between the experiment and ANN (4-2-2-1) is 14.4% with R= 0.99965for training and R = 0.99183 for the test as in the Fig.12.
Comparison between the experiment data and the structure of the neural networks (ANN) on which the training was conducted (4-9-9-1) the average percentage of thermal efficiency difference between the experiment and ANN is 9.45% with R = 0.9997 for training and R = 0.99998 for testing as in the Fig.13.

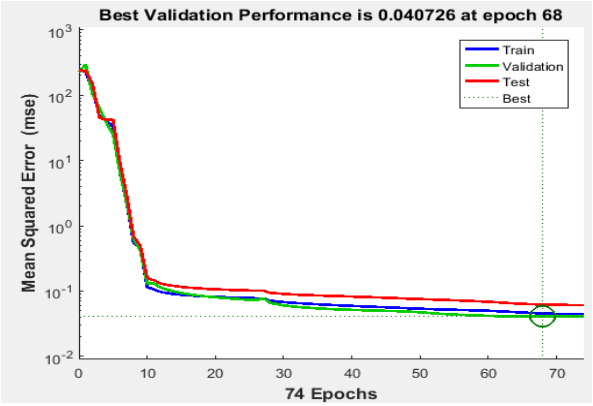

Figure10. Best validation performances in thermal efficiency structure 4-2-2-1.

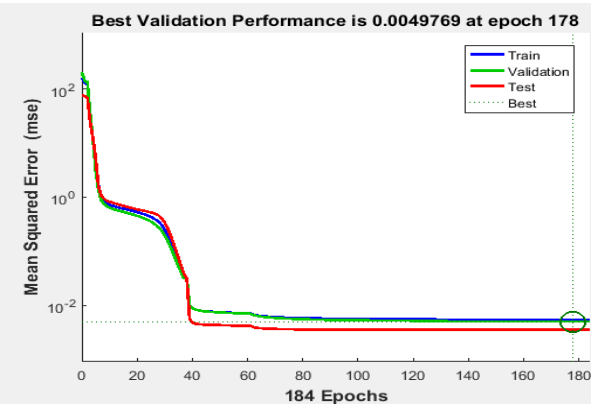

Figure 11. Best validation performances in thermal efficiency structure 4-9-9-1

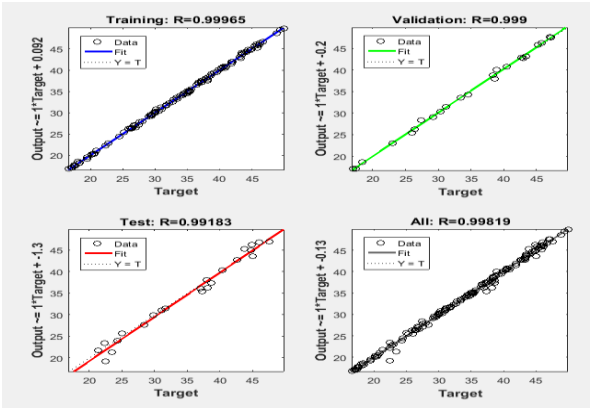

Figure12. Regression plot for structure (4-2-2-1).

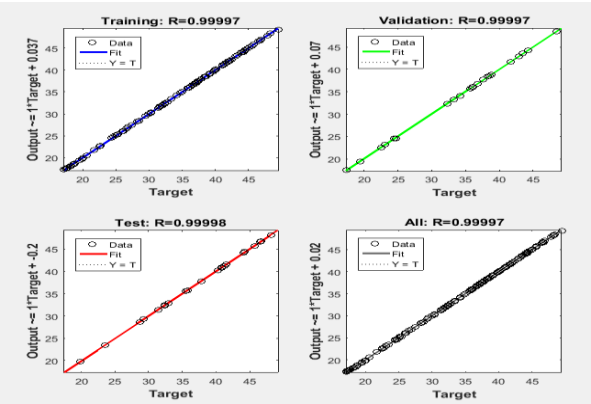

Figure13. Regression plot for structure (4-9-9-1).

Fig.14 represents the graph of the actual and expected Thermal efficiency values for the two neural network models used in this experiment. It is noted that the models (4-2-2-1) and (4-9-9-1) have similar behavior to the experimental line.

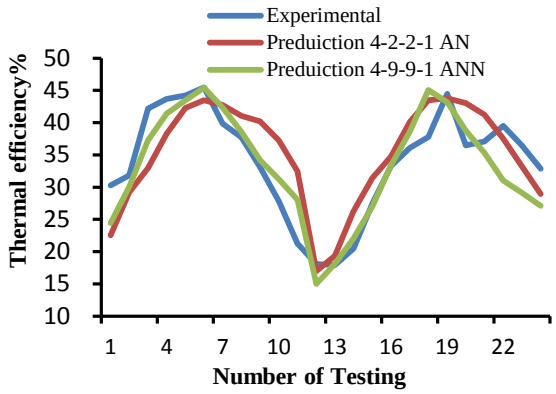

Figure 14. Investigation of the similarity of the line pattern between the experimental phase and the ANN of the test phase.

According to the reduced MSE and R-value, the model's performance improves when employing trials with a different number of neurons and a different algorithm as shown in Table 5.

Table 5. Values of the ANN structures in the training, validation, testing phases and the all data.

	4-2-2-1				4-9-9-1			
Set	Training	Validation	Testing	all data	Training	Validation	Testing	all data
RMSE	5.29	2.16	5.27	4.40	5.53	3.39	3.95	4.60
R^2	0.98	0.99	0.97	0.98	0.97	0.99	0.98	0.98
MSE	28.0	4.69	27.8	19.3	30.6	11.5	15.6	21.2

7- Conclusion

In this paper, an experimental study of the solar collector PTCS was carried out using different types of working fluids. Artificial neural networks have been used to predict the thermal efficiency of the system and the following can be concluded:

- The maximum increase in thermal efficiency of TiO_2/H_2O and CuO/H_2O compared to water was 7.12% and 19.2%, respectively.
- The thermal efficiency prediction results between experimental data and artificial neural network models are convergent and more reliable. The results showed that the agreement in thermal efficiency between the ANN analysis and the experimental results is about 91% for 4-9-9-1 and 86% for 4-2-21.
- The prediction of the thermal efficiency of the thermal solar collector for model 4 9 9 1 is more accurate and reliable than the prediction results for model 4-2-2-1.

Nomenclature

English Symbols			W_a	Aperture width	m
A_a	collector aperture area	m^2	W_P	weight nanoparticles	g
A_c	cross-sectional area of the flow	m^2	**Greek letters**		
A_{ri}	Inner surface area of the receiver	m^2			
A_s	Surface area of the concentrator	m^2	μ	Viscosity of working fluid	N.s /m^2
C_p	Specific heat capacity of water	J/kg.°C	η	Thermal efficiency	-
d_{ri}	Inner diameter of absorber tube	m	ρ	Fluid density	kg/m^3
d_{ro}	Outer diameter of absorber	m	φ	volume concentration	-
H_p	Height of the parabola	m	**Subscripts**		
I	Direct beam solar irradiation	W/m^2	r_i	Inner receiver.	
K	Thermal conductivity of fluid	W/m. °C	r_o	Outer receiver.	
L	Length of absorber tube	m	out	Outlet.	
$\dot{m}$	Mass flow rate	kg/s	in	Inlet.	
Q_a	Solar energy	W	m	Mean.	
Q_u	Useful heat gain	W	**Abbreviation**		
Re	Reynolds number	-	ANN	Artificial neural network	
T_{in}	Inlet temperature	°C	PTSC	Parabolic trough solar collector	
T_{out}	Outlet temperature	°C	RMSE	Root mean square error	
T_r	Surface temperature absorber	°C	RPF	Radial Basis Function	
U_m	Velocity of fluid	m/s	R^2	Maximum correlation coefficient	
$\dot{V}$	Volumetric flow rate	m^3/s	SWH	Solar water heating.	

References

[1] Urmee T, Walker E, Bahri PA, Baverstock G, Rezvani S, Saman W. Solar water heaters uptake in Australia-Issues and barriers. Sustain Energy Technol Assess 2018; 30:11–23.

[2] Navas J, Sánchez-Coronilla A, Martín EI, Teruel M, Gallardo JJ, Aguilar T, et al. On the enhancement of heat transfer fluid for concentrating solar power using Cu and Ni nanofluids: an experimental and molecular dynamics study. Nano Energy 2016; 27:213–24.

[3] Jin H, Lin G, Bai L, Zeiny A, Wen D. Steam generation in a nanoparticle-based solar receiver. Nano Energy 2016; 28:397–406.

[4] Assari MR, Tabrizi HB, Savadkohy M. Numerical and experimental study of inletoutlet locations effect in horizontal storage tank of solar water heater. Sustain Energy Technol Assess 2018; 25:181–90.

[5] Safarzadeh H, Sadeghi G, , Ameri Mehran. Experimental and numerical investigations on performance of evacuated tube solar collectors with parabolic concentrator, applying synthesized Cu2O/distilled water nanofluid. Energy Sustain Dev 2019; 48:88–106.

[6] Potenza M, Milanese M, Colangelo G, de Risi A. Experimental investigation of transparent parabolic trough collector based on gas-phase nanofluid. Appl Energy 2017; 203:560–70.

[7] Favale E, Colangelo G, Milanese M, de Risi A, Laforgia D. Cooling of electronic devices: nanofluids contribution. Appl Therm Eng 2017; 127:421–35.

[8] Milanese M, Iacobazzi F, Colangelo G, Lomascolo M, de Risi A. An explanation of the Al_2O_3 nanofluid thermal conductivity based on the phonon theory of liquid. Engineering 2016; 116:786–94.

[9] Boukelia T, Arslan O, Mecibah M. Potential assessment of a parabolic trough solar thermal power plant considering hourly analysis: ANN-based approach. Renew Energy 2017; 105:324–33.

[10] Kalogirou SA. Prediction of flat-plate collector performance parameters using artificial neural networks. Sol Energy 2006; 80(3):248–59.

[11] Buratti C, Barbanera M, Palladino D. An original tool for checking energy performance and certification of buildings by means of Artificial Neural Networks. Appl Energy 2014; 120:125–32.

[12] Tomy AM, Ahammed N, Subathra M, Asirvatham LG. Analysing the performance of a flat plate solar collector with silver/water nanofluid using artificial neural network. Procedia Comput Sci 2016; 93:33–40.

[13] Mahian O, Kianifar A, Heris SZ, Wongwises S. First and second laws analysis of a minichannel-based solar collector using boehmite alumina nanofluids: effects of nanoparticle shape and tube materials. Int J Heat Mass Transf 2014; 78:1166–76.

[14] [57] S. Ahmad, S. Abdullah and K. Sopian, "A review on the thermal performance of nanofluid inside circular tube with twisted tape inserts", Advances in Mechanical Engineering 2020, 12(6) 1–26.

[15] S. Ahmad, S. Abdullah and K. Sopian. A review on the thermal performance of nanofluid inside circular tube with twisted tape inserts. Advances in Mechanical Engineering 2020; 12:6 1–26.

[16] H. A. Mohammed, A. N. Al-Shamani, and J. M. Sheriff. Thermal and hydraulic characteristics of turbulent nanofluids flow in a rib-groove channel. Int. Commun. Heat Mass Transf 2012; 39:101584–1594.

[17] E. Bellos & Ch. Tzivanidis. Investigation of a star flow insert in a parabolic trough solar collector. Applied Energy 224 2018; 224: 86–102.

[18] Muhamed, Nura Mu'az, Sidik and Nor Azwadi Che. Utilisation of Nanofluids in Minichannel for Heat Transfer and Fluid Flow Augmentation. J. Adv. Res. Design 2018; 51:118-45.

[19] Gh. Sadeghi, S. Nazari, M. Ameri and F. Shama. Energy and exergy evaluation of the evacuated tube solar collector using Cu2O/water nanofluid utilizing ANN methods. Sustainable Energy Technologies and Assessments 2020; 3: 100578.

[20] S. Staub, E. Karaman, S. Kaya, H. Karapinar and E. Güven, "Artificial Neural Network and Agility", Procedia - Social and Behavioral Sciences 195 (2015) 1477 – 1485.

[21] ZURADA, Jacek M. Introduction to artificial neural systems. St. Paul: West, 1992

[22] CHEN, C. R.; RAMASWAMY, H. S.; MARCOTTE, M. Neural network applications in heat and mas. s transfer operations in food processing. WIT Trans State-of-the-art in Sci Eng, 2007, 13: 39-59.

[23] DERTAT, Arden. Applied deep learning-part 1: Artificial neural networks, 2017. URl:

https://towardsdatascience. com/applied-deep-learningpart-1-artificial-neural-networks-d7834f67a4f6, 2018.

[24] Zhang, G., Patuwo, B.E. & Hu, M.Y. 1998. Forecasting with artificial neural networks, the state of the art. International Journal of Forecasting14: 35-62.

[25] M. Al Shamisi, A. Assi and H. Hejase. Using MATLAB to Develop Artificial Neural Network Models for Predicting Global Solar Radiation in Al Ain City – UAE. Engineering Education and Research Using MATLAB 2011; 219-238.

[26] B. Caldo. Fuzzy logic derivation and simulation of a three-variable solar water heater using matlab fuzzy logic toolbox. Presented at the DLSU Research Congress 2015; 3: 1-6.